ACS Macro Letters

Letter

Cite This: ACS Macro Lett. 2019, 8, 905−911

pubs.acs.org/macroletters

Conformational State Hopping of Knots in Tensioned Polymer Chains

Beatrice W. Soh,[†] Alexander R. Klotz,[†] Liang Dai,[‡] and Patrick S. Doyle*,[†]

[†]Department of Chemical Engineering, Massachusetts Institute of Technology, Cambridge, Massachusetts 02139, United States

[‡]Department of Physics, City University of Hong Kong, 83 Tat Chee Avenue, Kowloon, Hong Kong, China

Supporting Information

ABSTRACT: We use Brownian dynamics simulations to study the conformational states of knots on tensioned chains. Focusing specifically on the 8_1 knot, we observe knot conformational state hopping and show that the process can be described by a two-state kinetic model in the presence of an external force. The distribution of knot conformational states depends on the applied chain tension, which leads to a force-dependent distribution of knot untying pathways. We generalize our findings by considering the untying pathways of other knots and find that the way knots untie is generally governed by the force applied to the chain. From a broader perspective, being able to influence how a knot unties via external force can potentially be useful for applications of single-molecule techniques in which knots are unwanted.

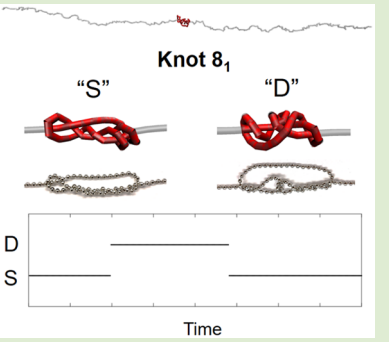

The prevalence of knots in our everyday experiences, be it in the form of entangled electric cords or hair, suggests that knots are a common occurrence. Indeed, it has been proven that the knotting probability of a chain tends to unity as the chain length approaches infinity,[1] hence, it is inevitable that knots are present on long chains. Although knots are mathematically well-defined only in circular chains,[2] linear chains with free ends can contain localized knots. Knots are encountered not only at the macroscale, but also on the microscale, having been observed in biopolymers such as DNA[3,4] and proteins,[5,6] as well as in synthetic polymers.[7]

The presence of knots has been shown to have consequences in a wide range of systems, from impairing the translocation of proteins through cellular membranes[8,9] to blocking DNA replication and transcription.[10] Hence, there has been growing interest in investigating the polymer dynamics of knotted chains. Previous studies by our group and others have considered problems such as the motion of knots along tensioned chains,[11−17] stretching of knotted polymers,[18−21] and spontaneous knotting on linear chains with free ends.[22−24] From the perspective of practical applications in biotechnology and nanotechnology, knots on biopolymers can introduce complexities. For example, knots can reduce the accuracy of next-generation genomics technologies, such as nanochannel genome mapping that relies on uniform stretching of molecules to convert physical distances between markers to genomic distances[25−27] and nanopore sequencing, which determines DNA sequences by measuring the ionic current blockade as molecules pass through the nanopore.[28,29]

The impact of knots on polymers has led to growing interest in not only the knotting of polymers, but also the untying of knots on polymers with free ends. Furthermore, there is gradual recognition of the importance of knotted protein structures and the links to neurodegenerative diseases,[30−33] and understanding how knots untie can complement studies on how knotted proteins fold. Most unknotting studies to date have focused on the mechanism of the untying process and unknotting dynamics,[22,34−37] with little attention given to the knot untying pathway, that is, the topological pathway of a knot untying. There is emerging interest in studying the simplification of topological states by Topoisomerase-II action to understand the mechanism of the enzyme, which serves to disentangle DNA via strand passage.[38−40] Since the way in which a knot unties is governed by the conformational state of the knot when it reaches a chain end, a study on knot conformational states is relevant to understanding how knots untie. A given knot can assume different conformational states that can be smoothly deformed into one another by changing the relative location of some strands without changing the knot type. In this study, we use Brownian dynamics simulations to study knot conformational states on tensioned chains. We choose to focus first on a specific knot, the 8_1 knot, and then generalize our findings to other knots. The 8_1 knot was selected due to it being sufficiently rich for multiple untying pathways, yet at the same time being a tractable model to study.

We used a Brownian dynamics approach to simulate the polymer as a linear, touching-bead chain with $N = 300$ beads of diameter b, connected by $N - 1$ rigid rods of length $l = b = 10$ nm (Figure 1a). We enforced constant bond

Received: June 18, 2019
Accepted: July 9, 2019

DOI: 10.1021/acsmacrolett.9b00462
ACS Macro Lett. 2019, 8, 905−911

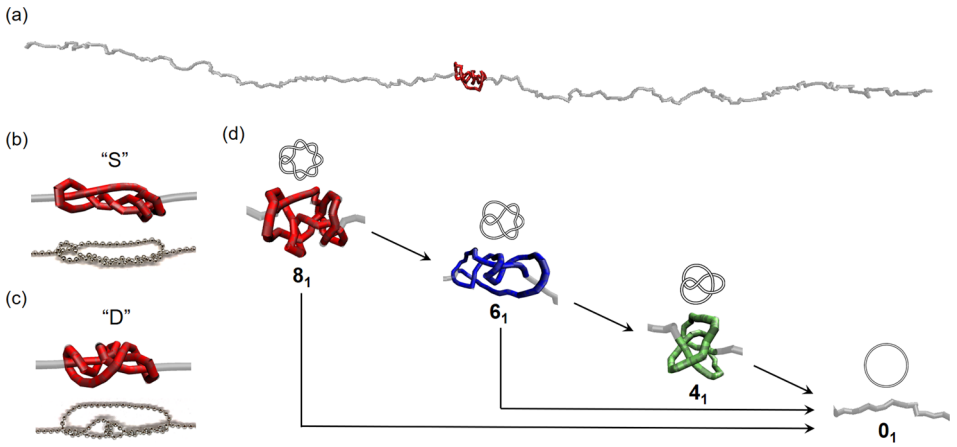

Figure 1. (a) Schematic of simulation setup: polymer chain with a 8_1 knot (red) held at constant tension. (b, c) Two conformational states for a 8_1 knot. Top: simulation snapshots. Bottom: images of macroscale chains. (d) Possible untying pathways for a 8_1 knot.

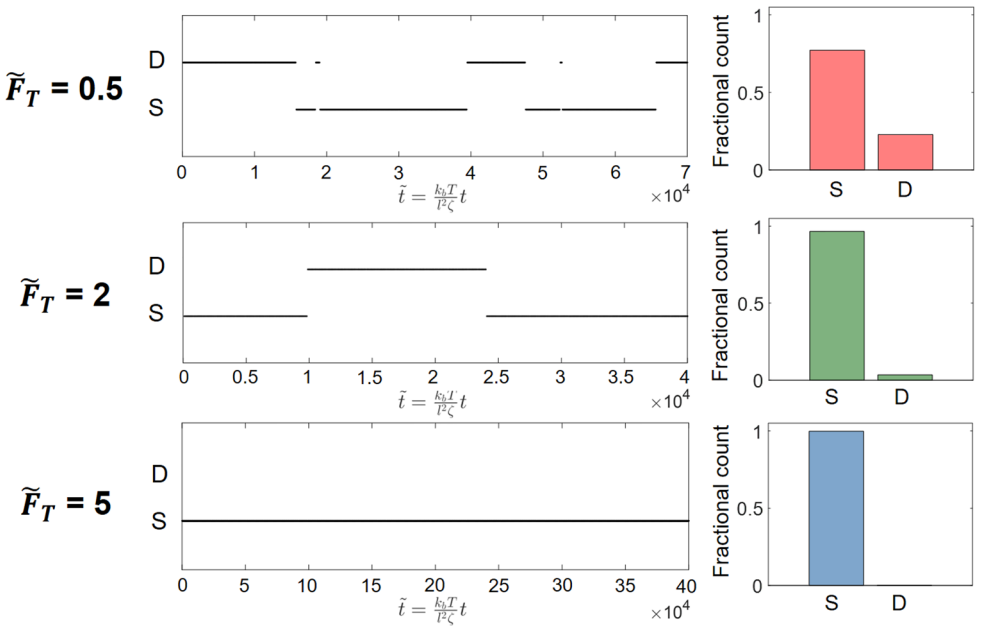

Figure 2. (Left) Knot conformational state versus time from representative simulation trajectories of initially centered 8_1 knots held under constant tensions $\tilde{F}_T = F_T/k_bTl$. (Right) Distributions of knot conformational states for the 8_1 knot held at constant tensions $\tilde{F}_T$. An ensemble of 50 chains was run for each $\tilde{F}_T$.

lengths and implemented short-range repulsion between chain segments to prevent self-crossings. Hydrodynamic interactions were neglected in this work, as in previous studies,[13,16] so the drag coefficient on each bead is ζ. In the simulations, we tied a knot into the center of the polymer chain and applied a constant tension force F_T at the chain ends. For a given set of simulation parameters, the knotted chains were equilibrated at the simulation conditions for at least $t = 10^5\tau_d$, where $\tau_d = l^2\zeta/k_bT$ is the characteristic rod diffusion time. During equilibration, the knot positions were held at the chain center via reptation moves. After equilibration, we ran the simulations until the knot fully untied from the chain, using a time step of $5 \times 10^{-4}\tau_d$. See the Supporting Information (SI) for details of the simulations and a representative simulation movie.

To determine the topology of linear chains, we first closed the chains into a ring with an auxiliary arc by implementing the minimally interfering closure scheme, in which the auxiliary arc is constructed to minimize additional entanglement that may be introduced during chain closure.[41] The chain topology was then determined by projecting the chain onto a plane parallel to the extension axis, identifying all chain crossings and calculating the Alexander polynomial.[42]

This study focused primarily on the 8_1 knot, which can take on two conformational states termed "S" (single clasp) and "D" (double clasp; Figure 1b,c). Depending on the knot conformational state and which end the knot unties from, the 8_1 knot can either completely untie in one step or partially untie into the 6_1 knot (Figure 1d). To determine the conformational state of the knot, we first identified the knot boundaries by finding the smallest subset of the chain that retained the topology of the entire chain via calculation of the Alexander polynomial. Next, we took the crossing on one end of the knot boundary and switched it from over to under or vice versa, an operation known as a crossing switch and equivalent to looping a chain end through the knot once, or untying one step of the knot. We then determined the topology of the chain resulting from the crossing switch by computing the Alexander polynomial. By repeating the same

DOI: 10.1021/acsmacrolett.9b00462
ACS Macro Lett. 2019, 8, 905−911

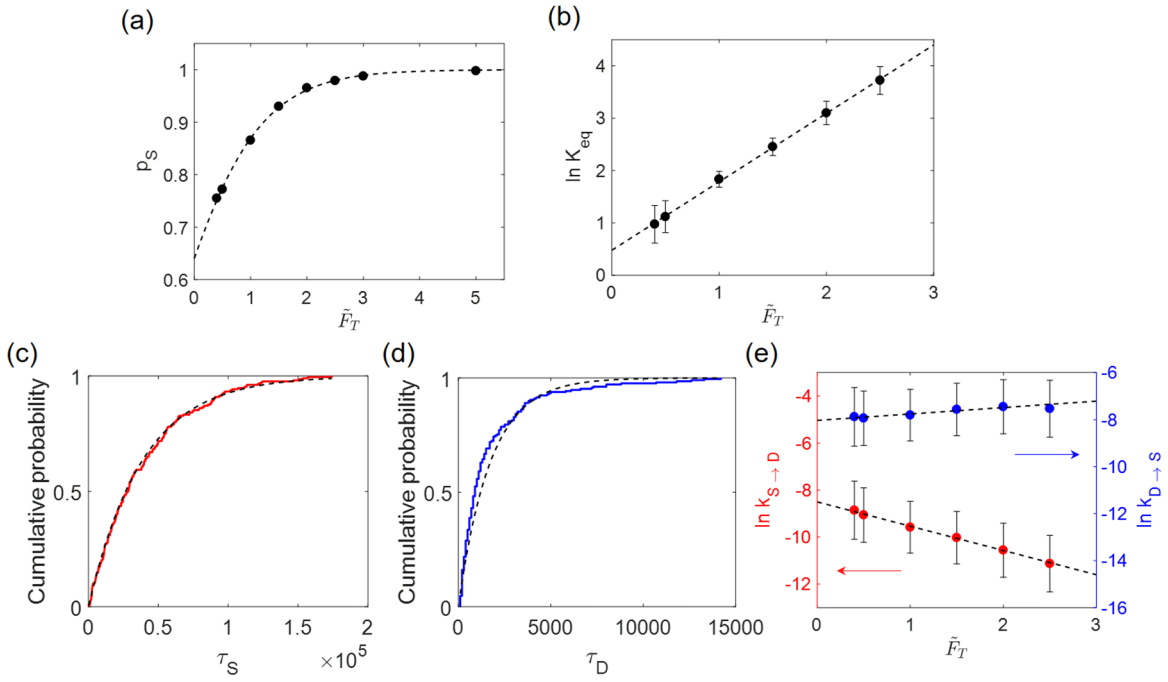

Figure 3. (a) Probability of a 8_1 knot being in the "S" conformational state, p_S, as a function of chain tension $\tilde{F}_T$. Dashed line is best fit to probability of a two-state system, given by eq 2. (b) Logarithm of the equilibrium constant K_{eq} as a function of chain tension $\tilde{F}_T$. Dashed line is fit to eq 4. (c, d) Cumulative distribution of dwell times in the "S" (red) and "D" (blue) conformational states for $\tilde{F}_T = 2$. Dashed lines are exponential fits to the distributions. (e) Logarithm of the rate constants $k_{S\to D}$ (red) and $k_{D\to S}$ (blue). Dashed lines are fits to eq 5. Error bars represent 95% confidence intervals.

procedure with a crossing switch on the other end of the knot boundary, we were able to obtain the knot conformational state. To illustrate this procedure with a 8_1 knot in the "S" conformational state shown in Figure 1b, a crossing switch on the left boundary of the knot would result in a 0_1 knot, or unknot, and a crossing switch on the right boundary would give a 6_1 knot (see Figure S1 in the SI). Since the detected knot boundaries and, consequently, the detected knot conformational state can be dependent on how the chain crossings are projected onto the chosen plane, we performed crossing switches on knot boundaries with the knot projected onto 200 different planes and selected the most frequently detected conformational state at each time step. See the SI for additional details regarding the knot conformational state detection algorithm.

A knot on a chain held under constant tension undergoes diffusive motion along the chain and unties upon reaching a chain end.[11,13,14,16] One might expect that the conformational state of a knot depends solely on how the knot was tied onto the chain. To determine if this is the case, we tied 8_1 knots in the "D" conformational state onto tensioned chains and tracked the knot conformational states on equilibrated chains. We show in Figure 2 (left panel) representative traces of knot conformational state over time as initially centered 8_1 knots diffuse along chains subjected to constant tension forces, from which we make two key observations. First, we observe hopping between the "S" and "D" conformational states, which shows that thermal fluctuations are able to induce conformational rearrangements of the knot. Therefore, the conformational state of a knot on a tensioned chain is not simply determined by its initial state. We note that there is fast equilibration of conformational states following hopping events. Second, the greater the chain tension, the fewer the occurrences of conformational state hopping and the shorter the durations spent in the "D" conformational state. Evidently, there is a force-dependent probability of the knot being in a given conformational state. Figure 2 (right panel) shows the distributions of knot conformational states for 8_1 knots on equilibrated chains under constant tensions. As was observed qualitatively from the individual traces, the 8_1 knot predominantly assumes the "S" conformational state within the range of chain tensions investigated, with the time spent in the "S" conformational state increasing with increasing tension. We point out that the knots studied in this work are fully equilibrated; the distributions of knot conformational states are independent of the initial state (Figure S7).

We postulate that the conformational states of the 8_1 knot on a tensioned chain can be described as a two-state system in the presence of an external force. The application of force introduces a well-defined mechanical reaction coordinate for the process—end-to-end distance of the chain—and allows the energy diagram of the system to be described in terms of chain extension.[43] The "S" and "D" conformational states are associated with local free energy minima at positions r_S and r_D along the reaction coordinate, respectively. The partition function of a system at fixed temperature T, pressure P, and force F_T is given by

$$Z = \sum_i \exp\left(-\frac{\Delta G_i - F_T r_i}{k_B T}\right) \tag{1}$$

where G_i is the free energy of state i and r_i is the extension of state i. For a two-state system, the probability of the knot being in each state is thus

$$p_S = \frac{1}{1 + \exp\left(\frac{\Delta G - F_T \Delta r}{k_B T}\right)} \tag{2}$$

DOI: 10.1021/acsmacrolett.9b00462
ACS Macro Lett. 2019, 8, 905−911

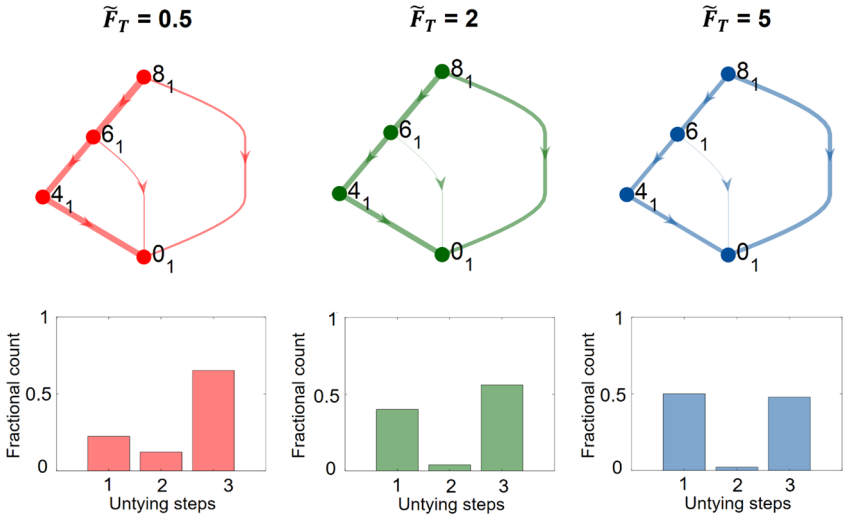

Figure 4. Distributions of untying pathways (top) and untying steps (bottom) for the 8_1 knot held at constant tensions $\tilde{F}_T$. The width of each untying pathway is weighted by the observed number of occurrences.

$$p_D = \frac{1}{1 + \exp\left(-\frac{\Delta G - F_T \Delta r}{k_B T}\right)} \tag{3}$$

where $\Delta G = G_S - G_D$ is the difference in free energy and $\Delta r = r_S - r_D$ is the difference in chain extension between the two states.

We compute the probability of the 8_1 knot being in the "S" conformational state, p_S, under a range of chain tensions (Figure 3a). By fitting p_S as a function of tension $\tilde{F}_T = F_T l/k_B T$ to eq 2, we obtain $\Delta G/k_B T = -0.578 \pm 0.052$ and $\Delta r/Nl = 0.0044 \pm 0.0002$. The difference in fractional extension between chains with a 8_1 knot in the "S" and "D" conformational states is determined from simulation data to be 0.0050 ± 0.0006 (Figures S8 and S9), in good agreement with the value of Δr extracted from the fit to eq 2. Indeed, the process of conformational state hopping appears to be well-described by a two-state model. The 8_1 knot can exist in either the "S" or "D" conformational state, with the small free energy difference ($<1\ k_B T$) implying an approximately equal distribution of conformational states in the absence of force, consistent with the extrapolated fit in Figure 3a. In the presence of a force, the "S" conformational state is favored due to the chain having a longer extension. By increasing the force applied to the chain, we shift the equilibrium between the two conformational states toward the "S" conformational state, a process similarly observed with protein and RNA unfolding.[44,45] The fast equilibration of conformational states during hopping events indicates that the potential wells at the "S" and "D" conformational states are deep and a large activation energy is required to overcome the barrier between the conformational states.

At a given force, the equilibrium constant between the "S" and "D" conformational states is given by

$$K_{eq} = \exp\left(-\frac{\Delta G - F_T \Delta r}{k_B T}\right) \tag{4}$$

and can be determined as the ratio of average dwell times of the knot in each conformational state. We plot ln K_{eq} as a function of chain tension $\tilde{F}_T$ (Figure 3b) and fit the data to eq 4 as a second, independent measure of ΔG and Δr. Doing so, we obtain $\Delta G/k_B T = -0.480 \pm 0.072$ and $\Delta r/Nl = 0.0044 \pm 0.0002$, consistent with values yielded from the fit to the probability of being in a given conformational state and within error of the value of Δr determined from simulation data.

To further probe the kinetics of the system, we consider the distribution of dwell times for the knot in each conformational state. The cumulative distributions of dwell times can be fit to exponential distributions (Figures 3c,d and S10), suggesting that the process of conformational state hopping at a given force is Markovian. We can extract rate constants $k_{S\to D}$ and $k_{D\to S}$ from single exponential fits to the data. From the dependence of the rate coefficients on applied force, we can then determine the distance between each conformational state and the transition state (see SI for derivation)

$$\frac{d \ln k}{d F} = \frac{\Delta r^\dagger}{k_B T} \tag{5}$$

where $\Delta r^\dagger$ is the average distance between the conformational state and transition state.[44] By plotting the dependence of the rate constants on the force applied (Figure 3e), we find $\Delta r_S^\dagger/Nl = 0.0034 \pm 0.0002$ and $\Delta r_D^\dagger/Nl = 0.0009 \pm 0.0005$. This indicates that the transition state is located much closer to the "D" than the "S" conformational state and implies that the rate of conformational state hopping from "D" to "S" is insensitive to the applied force. This is further supported by the plot of ln $k_{D\to S}$ versus $\tilde{F}_T$ being relatively flat (Figure 3e).

Having studied the process of conformational state hopping for the 8_1 knot, we now focus on how the knot unties when it reaches a chain end. Since the way in which a knot unties depends on the knot conformational state and the distribution of conformational states is governed by the chain tension, we expect the untying pathways of knots to also be dependent on the force applied to the chain.

The 8_1 knot can untie via the pathways shown in Figure 1d. From the "S" conformational state, the knot can either completely untie in one step or partially untie into the 6_1 knot; from the "D" conformational state, the knot partially unties into the 6_1 knot regardless of which chain end loops through the knot (see Figures S11 and S12 for detailed untying pathways). We highlight that the partially untied 6_1 knot can also undergo conformational state hopping and different

DOI: 10.1021/acsmacrolett.9b00462
ACS Macro Lett. 2019, 8, 905−911

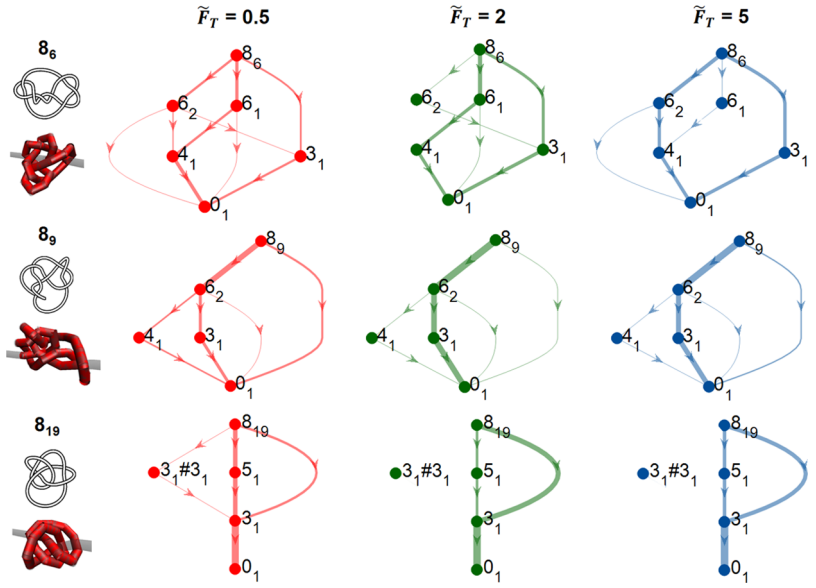

Figure 5. Distributions of untying pathways for the 8_6 knot (top), 8_9 knot (middle) and 8_{19} knot (bottom) held at constant tensions $\tilde{F}_T$. The width of each untying pathway is weighted by the observed number of occurrences.

untying pathways, hence the untying pathway of the 8_1 knot is not solely determined by the knot conformational state and chain end that the knot comes off. Figure 4 shows the distributions of untying pathways for the 8_1 knot across a range of applied forces (see Table S1 for data). We observe an evident shift in untying pathways as the chain tension increases from $\tilde{F}_T$ = 0.5 to $\tilde{F}_T$ = 5. When $\tilde{F}_T$ = 0.5, the 8_1 knot mostly unties via the 6_1 knot (~75%), which leads to a multistep untying process. This is in agreement with the knot having a ~20% probability of being in the "D" conformational state (Figure 2). On the other hand, when $\tilde{F}_T$ = 5, the 8_1 knot either completely unties to the unknot or partially unties to the 6_1 knot with equal likelihood, consistent with the knot having almost 100% probability of being in the "S" conformational state. By changing the force applied to the knotted chain, we can influence the untying pathway and number of steps needed to completely untie the knot.

Up to this point, we have studied extensively the kinetics of the conformational state hopping process and implications for the knot untying pathway for a specific knot, the 8_1 knot. The question that then arises is, do we observe a similar phenomenon with other knots? While it is laborious to investigate all possible conformational states for other knots, we can generalize our findings by considering the untying pathways of various knots across a range of chain tensions. Although we do not track the conformational states of these knots along the chains, we can gain some insight from the untying pathways exhibited by the knots. First, other than $(p,2)$-torus knots that untie only via one pathway, a given knot that does not undergo conformational state hopping is expected to untie by one of two pathways, depending on which end of the chain the knot comes off. Conversely, if a knot exhibits more than two untying pathways, conformational state hopping must have occurred. Second, we expect any effect of applied force on tilting the energy landscape and changing the knot conformational state distribution to manifest in a force-dependent distribution of the untying pathways. We choose three other knots with sufficient complexity for rich unknotting dynamics—the 8_6, 8_9 and 8_{19} knots—and study the untying pathways (see SI for justification). We point out that the 8_{19} knot is a prime knot that can untie into a composite knot $(3_1\#3_1)$. Figure 5 shows the distributions of untying pathways for the 8_6, 8_9 and 8_{19} knots for applied forces from $\tilde{F}_T$ = 0.5 to $\tilde{F}_T$ = 5 (see Tables S2–S4 for data). We observe that all three knots exhibit more than two untying pathways, which indicates that conformational state hopping occurred. Furthermore, we generally observe shifts in the preferred untying pathways with changes in the applied chain tensions. Specifically, with increasing chain tension, the frequency of the 8_6 knot partially untying into the 3_1 knot increases, the 8_9 knot increasingly undergoes multistep untying via the 6_2 knot and the 8_{19} knot increasingly unties into the 3_1 knot over the 5_1 and $3_1\#3_1$ knots. Hence, we conclude that the force-dependent conformational state hopping behavior on tensioned chains is not unique to the 8_1 knot.

In this work, we studied the conformational states of the 8_1 knot on tensioned linear chains and showed that the knot can hop between different conformational states stochastically in a way that depends on the applied force, which in turn affects how the knot unties when it reaches a chain end. We expect that the way in which a knot unties has implications for the knot untying time and chain dynamics during the unknotting process. We generalized our findings to other knots by considering the untying pathways of various knots at a range of chain tensions. Although other knots might not exist in only two possible conformational states, in which case we can imagine invoking a multistate model to describe the kinetics of the conformational state hopping process, we generally observe a force-dependent distribution of knot untying pathways for the knots studied, suggesting that the conformational state hopping behavior in the presence of an external force is not specific to the 8_1 knot. From a practical standpoint, being able to direct the untying pathway of a knot via external force can be useful for applications of single-molecule techniques in which knots are undesired, such as nanochannel genome mapping and direct linear analysis.[27] Moving forward, we hope that this work inspires further studies into the kinetics of knotted chains, for example in nonequilibrium flows.

DOI: 10.1021/acsmacrolett.9b00462
ACS Macro Lett. 2019, 8, 905−911

■ ASSOCIATED CONTENT

Supporting Information

The Supporting Information is available free of charge on the ACS Publications website at DOI: 10.1021/acsmacrolett.9b00462.

Simulation and knot conformational state detection algorithm details. Additional data analysis. Justification for selection of other knot types. Detailed untying pathways for the 8_1 knot (PDF)

Representative simulation movie of a chain with the 8_1 knot held under constant tension $\tilde{F}_T = 2$ (AVI)

■ AUTHOR INFORMATION

Corresponding Author

*E-mail: pdoyle@mit.edu.

ORCID

Beatrice W. Soh: 0000-0001-8399-5995
Alexander R. Klotz: 0000-0002-1581-6956
Liang Dai: 0000-0002-4672-6283
Patrick S. Doyle: 0000-0003-2147-9172

Notes

The authors declare no competing financial interest.

■ ACKNOWLEDGMENTS

We acknowledge Robert Scharein of KnotPlot for the knot diagrams. This work was supported by the National Science Foundation (NSF) Grant CBET-1602406. B.W.S. is funded by the Agency for Science, Technology and Research (A*STAR), Singapore.

■ REFERENCES

(1) Sumners, D. W.; Whittington, S. G. Knots in Self-Avoiding Walks. *J. Phys. A: Math. Gen.* **1988**, *21* (7), 1689−1694.
(2) Orlandini, E.; Whittington, S. G. Statistical Topology of Closed Curves: Some Applications in Polymer Physics. *Rev. Mod. Phys.* **2007**, *79* (2), 611−642.
(3) Liu, L. F.; Perkocha, L.; Calendar, R.; Wang, J. C. Knotted DNA from Bacteriophage Capsids. *Proc. Natl. Acad. Sci. U. S. A.* **1981**, *78* (9), 5498−502.
(4) Arsuaga, J.; Vázquez, M.; Trigueros, S.; Sumners, D. W.; Roca, J. Knotting Probability of DNA Molecules Confined in Restricted Volumes: DNA Knotting in Phage Capsids. *Proc. Natl. Acad. Sci. U. S. A.* **2002**, *99* (8), 5373−7.
(5) Nureki, O.; Shirouzu, M.; Hashimoto, K.; Ishitani, R.; Terada, T.; Tamakoshi, M.; Oshima, T.; Chijimatsu, M.; Takio, K.; Vassylyev, D. G.; Shibata, T.; Inoue, Y.; Kuramitsu, S.; Yokoyama, S. An Enzyme with a Deep Trefoil Knot for the Active-Site Architecture. *Acta Crystallogr., Sect. D: Biol. Crystallogr.* **2002**, *58*, 1129−37.
(6) Virnau, P.; Mirny, L. A.; Kardar, M. Intricate Knots in Proteins: Function and Evolution. *PLoS Comput. Biol.* **2006**, *2* (9), 1074−1079.
(7) Schappacher, M.; Deffieux, A. Imaging of Catenated, Figure-of-Eight, and Trefoil Knot Polymer Rings. *Angew. Chem., Int. Ed.* **2009**, *48* (32), 5930−5933.
(8) Szymczak, P. Tight Knots in Proteins: Can They Block the Mitochondrial Pores? *Biochem. Soc. Trans.* **2013**, *41* (2), 620−624.
(9) Szymczak, P. Translocation of Knotted Proteins Through a Pore. *Eur. Phys. J.: Spec. Top.* **2014**, *223* (9), 1805−1812.
(10) Portugal, J.; Rodriguez-Campos, A. T7 RNA Polymerase Cannot Transcribe Through a Highly Knotted DNA Template. *Nucleic Acids Res.* **1996**, *24* (24), 4890−4894.
(11) Bao, X. R.; Lee, H. J.; Quake, S. R. Behavior of Complex Knots in Single DNA Molecules. *Phys. Rev. Lett.* **2003**, *91* (26), 265506.
(12) Vologodskii, A. Brownian Dynamics Simulation of Knot Diffusion Along a Stretched DNA Molecule. *Biophys. J.* **2006**, *90* (5), 1594−7.
(13) Huang, L.; Makarov, D. E. Langevin Dynamics Simulations of the Diffusion of Molecular Knots in Tensioned Polymer Chains. *J. Phys. Chem. A* **2007**, *111* (41), 10338−10344.
(14) Matthews, R.; Louis, A. A.; Yeomans, J. M. Effect of Topology on Dynamics of Knots in Polymers Under Tension. *Europhys. Lett.* **2010**, *89* (2), 20001.
(15) Di Stefano, M.; Tubiana, L.; Di Ventra, M.; Micheletti, C. Driving Knots on DNA with AC/DC Electric Fields: Topological Friction and Memory Effects. *Soft Matter* **2014**, *10* (34), 6491−6498.
(16) Narsimhan, V.; Renner, C. B.; Doyle, P. S. Jamming of Knots Along a Tensioned Chain. *ACS Macro Lett.* **2016**, *5* (1), 123−127.
(17) Klotz, A. R.; Soh, B. W.; Doyle, P. S. Motion of Knots in DNA Stretched by Elongational Fields. *Phys. Rev. Lett.* **2018**, *120*, 188003.
(18) Farago, O.; Kantor, Y.; Kardar, M. Pulling Knotted Polymers. *Europhys. Lett.* **2002**, *60* (1), 53−59.
(19) Caraglio, M.; Micheletti, C.; Orlandini, E. Stretching Response of Knotted and Unknotted Polymer Chains. *Phys. Rev. Lett.* **2015**, *115* (18), 188301.
(20) Renner, C. B.; Doyle, P. S. Stretching Self-Entangled DNA Molecules in Elongational Fields. *Soft Matter* **2015**, *11* (16), 3105−3114.
(21) Soh, B. W.; Narsimhan, V.; Klotz, A. R.; Doyle, P. S. Knots Modify the Coil-Stretch Transition in Linear DNA Polymers. *Soft Matter* **2018**, *14*, 1689−1698.
(22) Tubiana, L.; Rosa, A.; Fragiacomo, F.; Micheletti, C. Spontaneous Knotting and Unknotting of Flexible Linear Polymers: Equilibrium and Kinetic Aspects. *Macromolecules* **2013**, *46* (9), 3669−3678.
(23) Dai, L.; Renner, C. B.; Doyle, P. S. Metastable Tight Knots in Semiflexible Chains. *Macromolecules* **2014**, *47* (17), 6135−6140.
(24) Dai, L.; Renner, C.; Doyle, P. S. Origin of Metastable Knots in Single Flexible Chains. *Phys. Rev. Lett.* **2015**, *114* (3), 037801.
(25) Lam, E. T.; Hastie, A.; Lin, C.; Ehrlich, D.; Das, S. K.; Austin, M. D.; Deshpande, P.; Cao, H.; Nagarajan, N.; Xiao, M.; Kwok, P.-Y. Genome Mapping on Nanochannel Arrays for Structural Variation Analysis and Sequence Assembly. *Nat. Biotechnol.* **2012**, *30* (8), 771−6.
(26) Reisner, W.; Pedersen, J. N.; Austin, R. H. DNA Confinement in Nanochannels: Physics and Biological Applications. *Rep. Prog. Phys.* **2012**, *75* (10), 106601.
(27) Dorfman, K. D.; King, S. B.; Olson, D. W.; Thomas, J. D. P.; Tree, D. R. Beyond Gel Electrophoresis: Microfluidic Separations, Fluorescence Burst Analysis, and DNA Stretching. *Chem. Rev.* **2013**, *113* (4), 2584−667.
(28) Rosa, A.; Di Ventra, M.; Micheletti, C. Topological Jamming of Spontaneously Knotted Polyelectrolyte Chains Driven Through a Nanopore. *Phys. Rev. Lett.* **2012**, *109* (11), 118301.
(29) Narsimhan, V.; Renner, C. B.; Doyle, P. S. Translocation Dynamics of Knotted Polymers Under a Constant or Periodic External Field. *Soft Matter* **2016**, *12* (22), 5041−5049.
(30) Taylor, W.R. A. Deeply Knotted Protein Structure and How It Might Fold. *Nature* **2000**, *406* (6798), 916−919.
(31) Bölinger, D.; Sułkowska, J. I.; Hsu, H.-P.; Mirny, L. A.; Kardar, M.; Onuchic, J. N.; Virnau, P. A Stevedore's Protein Knot. *PLoS Comput. Biol.* **2010**, *6* (4), No. e1000731.
(32) Ziegler, F.; Lim, N. C. H.; Mandal, S. S.; Pelz, B.; Ng, W.-P.; Schlierf, M.; Jackson, S. E.; Rief, M. Knotting and Unknotting of a Protein in Single Molecule Experiments. *Proc. Natl. Acad. Sci. U. S. A.* **2016**, *113* (27), 7533−7538.
(33) Wojciechowski, M.; Gómez-Sicilia, À.; Carrión-Vázquez, M.; Cieplak, M. Unfolding Knots by Proteasome-Like Systems: Simulations of the Behaviour of Folded and Neurotoxic Proteins. *Mol. BioSyst.* **2016**, *12* (9), 2700−2712.
(34) Micheletti, C.; Orlandini, E. Knotting and Unknotting Dynamics of DNA Strands in Nanochannels. *ACS Macro Lett.* **2014**, *3* (9), 876−880.

DOI: 10.1021/acsmacrolett.9b00462
ACS Macro Lett. 2019, 8, 905−911

(35) Renner, C. B.; Doyle, P. S. Untying Knotted DNA with Elongational Flows. *ACS Macro Lett.* **2014**, *3*, 963−967.
(36) Soh, B. W.; Klotz, A. R.; Doyle, P. S. Untying of Complex Knots on Stretched Polymers in Elongational Fields. *Macromolecules* **2018**, *51* (23), 9562−9571.
(37) Caraglio, M.; Baldovin, F.; Marcone, B.; Orlandini, E.; Stella, A. L. Topological Disentanglement Dynamics of Torus Knots on Open Linear Polymers. *ACS Macro Lett.* **2019**, 576−581.
(38) Flammini, A.; Maritan, A.; Stasiak, A. Simulations of Action of DNA Topoisomerases to Investigate Boundaries and Shapes of Spaces of Knots. *Biophys. J.* **2004**, *87* (5), 2968−2975.
(39) Stolz, R.; Yoshida, M.; Brasher, R.; Flanner, M.; Ishihara, K.; Sherratt, D. J.; Shimokawa, K.; Vazquez, M. Pathways of DNA Unlinking: A Story of Stepwise Simplification. *Sci. Rep.* **2017**, *7* (1), 12420.
(40) Ziraldo, R.; Hanke, A.; Levene, S. D. Kinetic Pathways of Topology Simplification by Type-II Topoisomerases in Knotted Supercoiled DNA. *Nucleic Acids Res.* **2019**, *47* (1), 69−84.
(41) Tubiana, L.; Orlandini, E.; Micheletti, C. Probing the Entanglement and Locating Knots in Ring Polymers: A Comparative Study of Different Arc Closure Schemes. *Prog. Theor. Phys. Suppl.* **2011**, *191*, 192−204.
(42) Vologodskii, A. V.; Lukashin, A. V.; Frank-Kamenetskii, M. D.; Anshelevich, V. V. The Knot Problem in Statistical Mechanics of Polymer Chains. *J. Exp. Theor. Phys.* **1974**, *66*, 2153−2163.
(43) Tinoco, I.; Bustamante, C. The Effect of Force on Thermodynamics and Kinetics of Single Molecule Reactions. *Biophys. Chem.* **2002**, *101−102*, 513−33.
(44) Liphardt, J.; Onoa, B.; Smith, S. B.; Tinoco, I.; Bustamante, C. Reversible Unfolding of Single RNA Molecules by Mechanical Force. *Science* **2001**, *292* (5517), 733−7.
(45) Cecconi, G.; Shank, E. A.; Bustamante, C.; Marqusee, S. Biochemistry: Direct Observation of the Three-State Folding of a Single Protein Molecule. *Science* **2005**, *309* (5743), 2057−2060.

DOI: 10.1021/acsmacrolett.9b00462
ACS Macro Lett. 2019, 8, 905−911